Biogeosciences

Southern Ocean phytoplankton under climate change: a shifting balance of bottom-up and top-down control

Tianfei Xue[1], **Jens Terhaar**[2,3,4], **A. E. Friederike Prowe**[1], **Thomas L. Frölicher**[3,4], **Andreas Oschlies**[1], and **Ivy Frenger**[1]

[1]GEOMAR Helmholtz Centre for Ocean Research Kiel, Kiel, Germany
[2]Department of Marine Chemistry and Geochemistry, Woods Hole Oceanographic Institution,
Woods Hole, Massachusetts, USA
[3]Climate and Environmental Physics, Physics Institute, University of Bern, Bern, Switzerland
[4]Oeschger Centre for Climate Change Research, University of Bern, Bern, Switzerland

Correspondence: Tianfei Xue (txue@geomar.de)

Abstract. Phytoplankton form the base of the marine food web by transforming CO_2 into organic carbon via photosynthesis. Despite the importance of phytoplankton for marine ecosystems and global carbon cycling, projections of phytoplankton biomass in response to climate change differ strongly across Earth system models, illustrating uncertainty in our understanding of the underlying processes. Differences are especially large in the Southern Ocean, a region that is notoriously difficult to represent in models. Here, we argue that total (depth-integrated) phytoplankton biomass in the Southern Ocean is projected to largely remain unchanged under climate change by the Coupled Model Intercomparison Project Phase 6 (CMIP6) multi-model ensemble because of a shifting balance of bottom-up and top-down processes driven by a shoaling mixed-layer depth. A shallower mixed layer is projected on average to improve growth conditions, consequently weaken bottom-up control, and confine phytoplankton closer to the surface. An increase in the phytoplankton concentration promotes zooplankton grazing efficiency, thus intensifying top-down control. However, large differences across the model ensemble exist, with some models simulating a decrease in surface phytoplankton concentrations. To reduce uncertainties in projections of surface phytoplankton concentrations, we employ an emergent constraint approach using the observed sensitivity of surface chlorophyll concentration, taken as an observable proxy for phytoplankton, to seasonal changes in the mixed-layer depth as an indicator for future changes in surface phytoplankton concentrations. The emergent constraint reduces uncertainties in surface phyto-

plankton concentration projections by around one-third and increases confidence that surface phytoplankton concentrations will indeed rise due to shoaling mixed layers under global warming, thus favouring intensified top-down control. Overall, our results suggest that while changes in bottom-up conditions stimulate enhanced growth, intensified top-down control opposes an increase in phytoplankton and becomes increasingly important for the phytoplankton response to climate change in the Southern Ocean.

1 Introduction

Phytoplankton are fundamental to the marine ecosystem and the global carbon cycle, as they are the base of the ocean food web (Pauly and Christensen, 1995) and account for approximately half of the global biological carbon fixation (Field et al., 1998). Despite the importance of phytoplankton for the carbon cycle and the future of marine ecosystems, the response of phytoplankton to climate change remains uncertain. Earth system model projections of phytoplankton biomass and its growth for the 21st century largely differ between models and scenarios (Steinacher et al., 2010; Laufkötter et al., 2015; Frölicher et al., 2016; Tagliabue et al., 2021), and even the direction of changes remains unclear (Kwiatkowski et al., 2020). The different projections are due to uncertainties in the underlying physical forcing and different biological and biogeochemical parameterisations of processes in the models (Laufkötter et al., 2015). Such differ-

ences in the biological and biogeochemical process parameterisations have the potential to propagate through the food web, often amplified by simplistic food web dynamics (Stock et al., 2014b), and cause even greater model differences for higher-trophic-level projections (Lotze et al., 2019). In turn, such differences in higher-trophic-level projections and simplistic food web dynamics will, through ill-constrained grazing pressure on phytoplankton, lead to amplified model differences in phytoplankton projections, forming a feedback loop for inter-model differences in simulated ecosystem dynamics. Given the role of phytoplankton in marine ecosystems and biogeochemical cycling, better constraining how phytoplankton respond to changes in their physical, chemical, and biological environment under climate change is critical.

Climate change affects phytoplankton through both "bottom-up" (Marinov et al., 2010; Leung et al., 2015) and "top-down" (Stock et al., 2014a; Kwiatkowski et al., 2019) control. Bottom-up control describes changes in phytoplankton growth due to changes in light, temperature, and nutrients caused by environmental factors like mixing or upwelling (Behrenfeld et al., 2006). Given that these environmental factors are projected to change under climate change, it is expected that phytoplankton will also be affected. Top-down control, on the other hand, refers to the impact of predators on phytoplankton populations. The major predator of phytoplankton is zooplankton. Phytoplankton changes are typically considered top-down controlled when zooplankton and phytoplankton changes are inversely related (Chust et al., 2014), for example, when phytoplankton decreases while zooplankton increases, suggesting that zooplankton are grazing down phytoplankton. Globally, changes in bottom-up control are thought to dominate the phytoplankton response to a changing climate, with increasing ocean stratification and shoaling mixed layers driving a reduction in nutrient supply and hence a reduction in phytoplankton biomass and growth (Sarmiento et al., 2004b; Bopp et al., 2005; Behrenfeld et al., 2006; Steinacher et al., 2010; Boyce et al., 2010). An opposite bottom-up response can be found in high-latitude regions where improved light conditions due to increased stratification and sea ice retreat are projected to lead to phytoplankton increases (Sarmiento et al., 2004b; Deppeler and Davidson, 2017). Although predators and grazing pressure also evolve with climate change (Shurin et al., 2012), top-down control has received much less attention (Ratnarajah et al., 2023).

The Southern Ocean is a region where models, albeit with an uncertain magnitude, robustly project that phytoplankton will grow better with shoaling mixed-layer depths under global warming (Figs. 1 and 2; Sarmiento et al., 2004b; Bopp et al., 2013; Laufkötter et al., 2015; Kwiatkowski et al., 2020). Despite the high abundance of macronutrients (Fig. A1), phytoplankton growth in the Southern Ocean is at present largely under bottom-up control by iron and light limitations (Martin et al., 1990; Mitchell et al., 1991; Arteaga

et al., 2020; Moore et al., 2013). Light limitation is especially strong in the Southern Ocean due to the deep mixed layers and low surface radiation in mid- to high-latitude winters. Under global warming, Southern Ocean phytoplankton growth conditions are anticipated to improve with rising temperatures and a prolonged growing season, as well as improving light conditions with increasing stratification, shoaling mixed-layer depths, and reduced sea ice cover (Bopp et al., 2001; Sarmiento et al., 2004b). Apart from the prominent limitation by light, changes in iron limitation in the Southern Ocean with climate change remain uncertain as the iron cycle is not well resolved mechanistically in Earth system models (Tagliabue et al., 2016). In addition to bottom-up control, top-down control via zooplankton also affects phytoplankton variability in the Southern Ocean (Le Quéré et al., 2016).

As phytoplankton in the Southern Ocean play an important role in the local food web and also in setting the biogeochemical characteristics of ocean waters globally, better understanding and constraining of their evolution under climate change is relevant for reliable projections of marine biological production well beyond the Southern Ocean (Sarmiento et al., 2004a; Marinov et al., 2006; Nissen et al., 2021). Here, we deliver crucial insights into phytoplankton projections under climate change, highlighting the dynamic interplay between bottom-up and top-down controls due to mixed-layer shoaling in the Southern Ocean. By employing an emergent constraint approach, we enhance our confidence in comprehending phytoplankton dynamics and their response to climate change.

2 Methods

2.1 Research area

This study focuses on the subantarctic and subpolar Antarctic regions, which approximately span the latitude range of 40–60° S (boxes in panel o of Figs. 1 and 2). This region has high levels of macronutrients sufficient to support the growth of phytoplankton and is relatively unaffected by sea ice. In the current climate, the seasonal change in mixed-layer depth (MLD) is known to be important for seasonal plankton dynamics, primarily because of its impact on light regulation (Arteaga et al., 2020).

2.2 Multi-model ensemble

Here we use the output of a multi-model ensemble (MME; Table 1) of 14 Earth system models (ESMs). Of the 14 models that we used, 13 ESMs are part of the Coupled Model Intercomparison Project Phase 6 (CMIP6; downloaded from https://esgf-data.dkrz.de, last access: 6 March 2024). The FOCI (Flexible Ocean and Climate Infrastructure; Chien et al., 2022) model run at GEOMAR (Helmholtz Centre for Ocean Research) was added to these 13 models. The selection of these models is based on the present availabil-
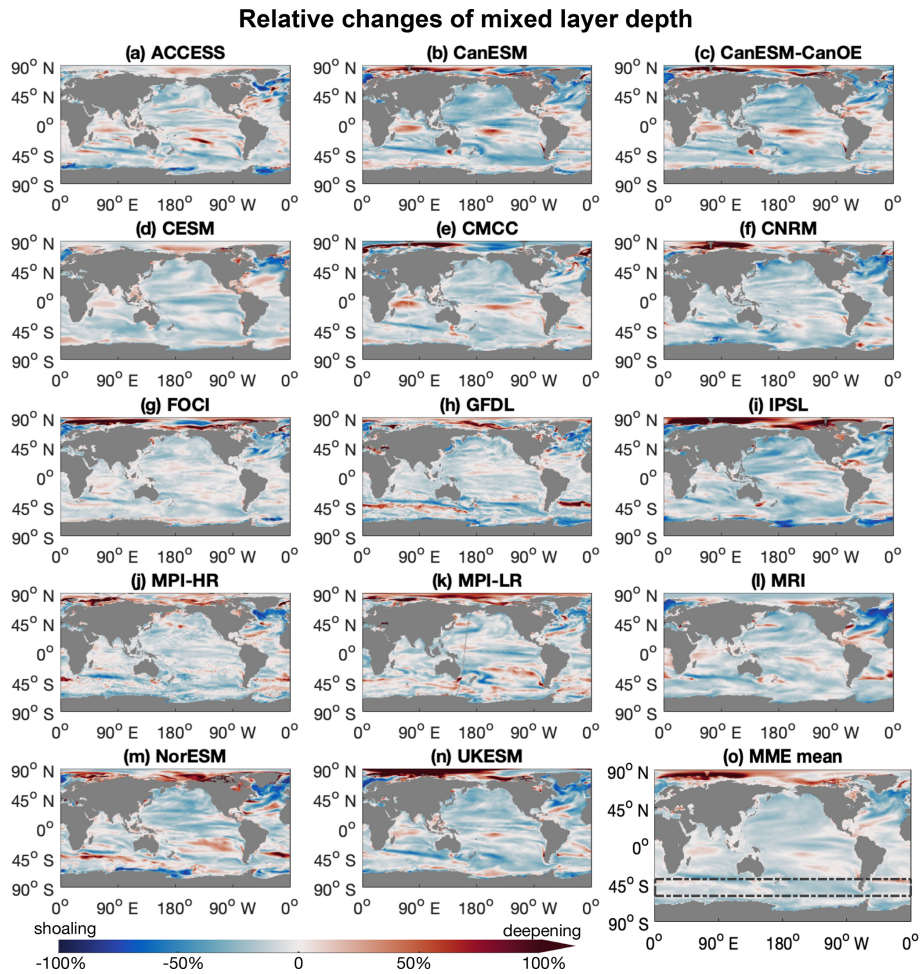
Relative changes of mixed layer depth

Figure 1. The mixed layers in the Southern Ocean are projected to shoal under a high-emission, no-mitigation scenario (SSP5-8.5). **(a–n)** Maps for individual climate models in a multi-model ensemble (MME; listed in Table 1), showing annual mean mixed-layer depth anomalies of the last decade (2090s) of the 21st century relative to the first decade (2000s), under the SSP5-8.5 scenario. **(o)** Mean of the multi-model ensemble. Boxes denoted by dashed lines mark the focus area. Red indicates deepening, and blue indicates shoaling mixed layers towards the end of the 21st century.

ity of the variables required (phytoplankton biomass concentration, zooplankton biomass concentration, mixed-layer depth, and surface chlorophyll concentration), the temporal resolution (monthly), and the experimental settings (historical simulation; piControl simulation to account for potential drifts; and the SSP5-8.5 (Shared Socioeconomic Pathway) high-emission, no-mitigation scenario). The models within the MME are structurally different and cover a range of different parameterisations of processes and initial conditions (Séférian et al., 2020). All output fields were regridded on a regular $1° \times 1°$ map using the bilinear interpolation of CDO (Climate Data Operators).

2.3 Emergent constraint

The emergent constraint approach is based on an identifiable relationship in a model ensemble between an observable con-

temporary sensitivity and an uncertain condition for future climates (Hall et al., 2019; Williamson et al., 2021). The observable contemporary condition can then be used to constrain future model projections, such as was previously done for the ocean carbon sink (Kessler and Tjiputra, 2016; Terhaar et al., 2021a, 2022), ocean acidification (Terhaar et al., 2020, 2021b), or marine primary productivity in the tropics (Kwiatkowski et al., 2017). Emergent constraints are often built upon relationships between the same variable at different times; e.g., Kwiatkowski et al. (2017) establish a link between the change in tropical primary production in response to temperature changes on interannual timescales and the change in tropical primary production in response to temperature changes over the 21st century. However, emergent constraints can also be built on relationships between different variables if these are mechanistically related; e.g., Terhaar et al. (2021a) used Southern Ocean sea surface salinity
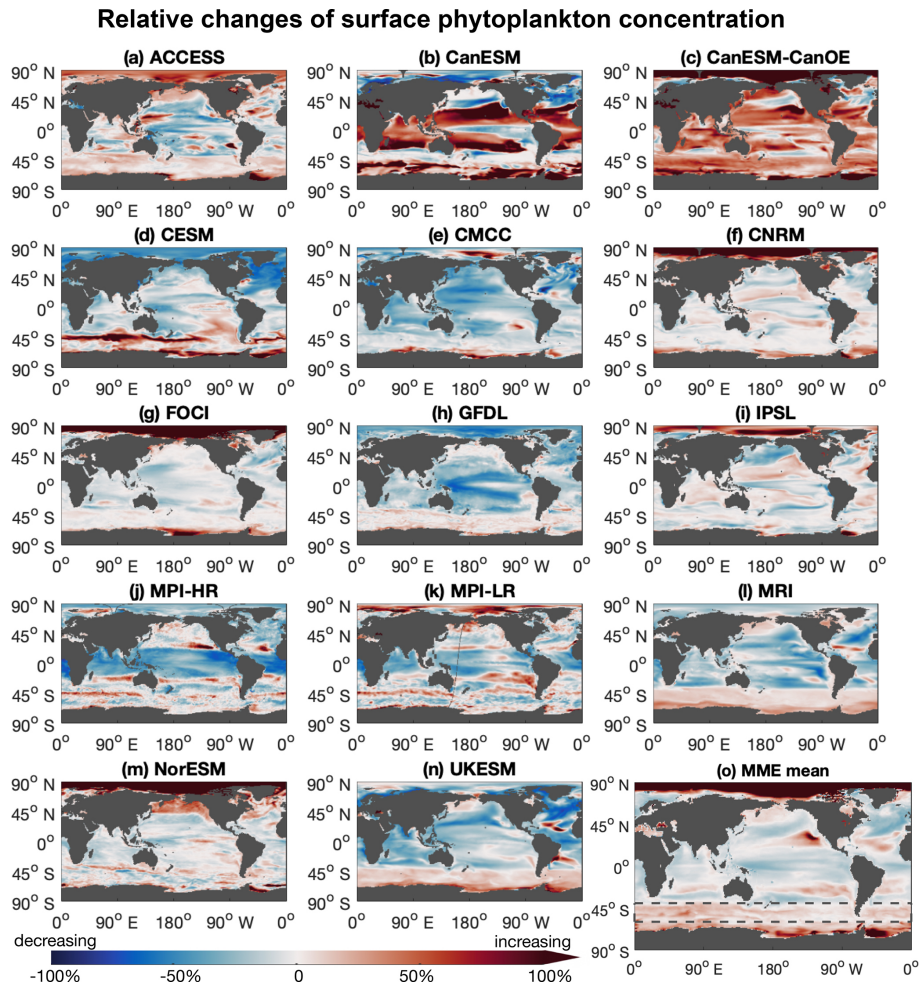
Relative changes of surface phytoplankton concentration

Figure 2. The Southern Ocean stands out as a region with projected increasing surface phytoplankton concentrations under a high-emission, no-mitigation scenario (SSP5-8.5). **(a–n)** Maps for individual climate models in a multi-model ensemble (MME; listed in Table 1), showing the relative change in surface phytoplankton of the last decade (2090s) of the 21st century relative to the first decade (2000s), under the SSP5-8.5 scenario. **(o)** Mean of the multi-model ensemble. Boxes denoted by dashed lines mark the focus area. Red indicates increasing, and blue indicates decreasing surface phytoplankton during the 21st century.

to constrain future uptake of anthropogenic carbon in that region because sea surface salinity determines sea surface density and hence the amount and mode of intermediate water formation.

Here, we apply the emergent constraint approach to reduce uncertainties in the projections of the long-term sensitivity of surface phytoplankton concentrations in the Southern Ocean to changes in the mixed-layer depth (S_{clm}; Eq. 2; period: 2000–2099) using contemporary seasonal sensitivities of surface chlorophyll concentrations, an observable proxy for surface phytoplankton concentrations with good spatiotemporal coverage from satellite-based sensors, to mixed-layer depth changes (S_{seas}; Eq. 1; period: 2000–2009). The emergent constraint we utilised here, incorporating distinct observable and constraint variables, hinges on the relationship between surface chlorophyll concentration and surface phytoplankton biomass concentration across individual mod-

els (Fig. A2). Benefiting from its comprehensive spatiotemporal coverage, chlorophyll provides an ideal balance by offering a strong linear correlation, easy observational access, and comparatively low observational uncertainties. For each of the individual models and for the observations, the respective contemporary seasonal sensitivity of surface chlorophyll concentrations to the MLD (S_{seas}) is computed as follows:

$$S_{seas} = \frac{(chl_{mmax} - chl_{mmin})/\overline{chl}}{(MLD_{mmax} - MLD_{mmin})/\overline{MLD}}, \qquad (1)$$

with overlines indicating the annual mean and mmax and mmin indicating the months with the minimum and maximum MLD that mark the beginning and the end of the shoaling period (shaded periods in Fig. 3). We explicitly selected the shoaling period, as the decrease due to MLD shoaling and improving light conditions are analogues to changes expected under global warming.

Table 1. Overview of the multi-model ensemble (MME) used in this study.

Label	Model name	Ocean biogeochemistry	Plankton groups	Simulations		Reference
				biomass	production	
(a)	ACCESS-ESM1.5	WOMBAT*	P1Z1	(✓)		Ziehn et al. (2020)
(b)	CanESM5	CMOC	P1Z1	✓		Swart et al. (2019)
(c)	CanESM5-CanOE	CanOE*	P2Z2	✓	✓	Christian et al. (2022)
(d)	CESM2-WACCM	MARBL*	P3Z1	✓		Danabasoglu et al. (2020)
(e)	CMCC-ESM2	BFM v5.2*	P2Z2	✓		Lovato et al. (2022)
(f)	CNRM-ESM2-1	PISCESv2-gas*	P2Z2	✓	✓	Séférian et al. (2019)
(g)	FOCI1	MOPS	P1Z1	✓	✓	Chien et al. (2022)
(h)	GFDL-ESM4	COBALTv2*	P3Z3	✓	✓	Dunne et al. (2020)
(i)	IPSL-CM6A-LR	PISCESv2*	P2Z2	✓		Boucher et al. (2020)
(j)	MPI-ESM1.2-HR	HAMOCC6*	P2Z1	✓	✓	Müller et al. (2018)
(k)	MPI-ESM1.2-LR	HAMOCC6*	P2Z1	✓	✓	Mauritsen et al. (2019)
(l)	MRI-ESM2.0	NPZD	P1Z1	✓		Tsujino et al. (2017)
(m)	NorESM2-MM	iHAMOCC*	P2Z1	✓		Tjiputra et al. (2020)
(n)	UKESM1-0-LL	MEDUSA*	P2Z2	✓	✓	Sellar et al. (2019)

* Indicates models that explicitly include iron limitation. PxZy in column "Plankton groups" indicates x phytoplankton and y zooplankton groups in the respective model. Column "Simulations" indicates models whose output was used in biomass- or production-relevant calculations. (✓) indicates model provides only surface value of phytoplankton biomass as output; therefore it is not used in the total plankton biomass analysis in Sect. 3.1.
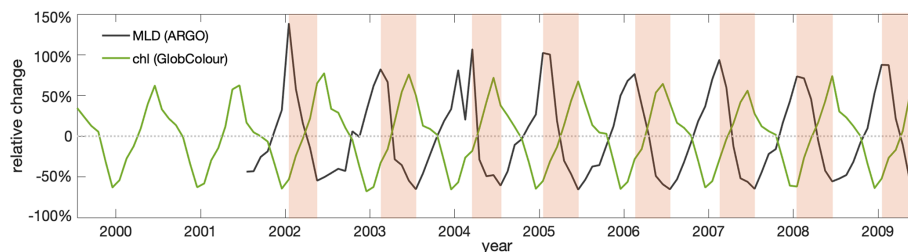

Figure 3. Observed surface chlorophyll (chl) concentration shows a clear seasonal cycle that, primarily, is anticorrelated with observed mixed-layer depths (MLDs). Contemporary seasonal variations relative to the respective annual means of observed MLD (Argo: black) and surface chlorophyll concentration based on merged satellite data (GlobColour: green) in the Southern Ocean subantarctic and subpolar Antarctic regions (40–60° S). The shaded areas indicate the seasonal MLD shoaling period.

Based on the strong correlation between projected surface chlorophyll and surface phytoplankton (Fig. A2), the long-term sensitivities of surface phytoplankton concentrations to mixed-layer changes (S_{clm}; Eq. 2) of individual models are calculated based on the relative changes in the surface phytoplankton concentration (R_{sphy}) and MLD (R_{MLD}) between the first decade (2000s) and the last decade (2090s) of the 21st century. The long-term sensitivity calculation here follows the definition of the seasonal sensitivity in Eq. (1).

$$S_{clm} = \frac{(\overline{sphy_{2090s}} - \overline{sphy_{2000s}})/\overline{sphy_{2000s}}}{(\overline{MLD_{2090s}} - \overline{MLD_{2000s}})/\overline{MLD_{2000s}}} = \frac{R_{sphy}}{R_{MLD}} \quad (2)$$

Relative MLD anomalies are used instead of absolute anomalies, as the relative anomaly relates to the dilution of phytoplankton across the mixed layer, which is one of the main mechanisms controlling surface phytoplankton concentration. Despite the large differences revealed in the absolute MLD and chlorophyll values of individual models (Fig. A3), the models resolve the same seasonal anticorrelation between

relative variations in MLD and chlorophyll as seen in observations (see results in Sect. 3.3.1).

The probability density functions (PDFs) of the long-term sensitivity (S_{clm}) were derived from a Gaussian distribution and the MME mean and standard deviation, assuming that all models have equal probability. We calculated the constrained PDFs following previous studies (Eq. 3; Eq. 20 in Williamson et al., 2021).

$$p(y) = \int_{-\infty}^{\infty} p(y \mid x) p(x) \mathrm{d}x$$

$$= \mathcal{N}\left(y \mid a + bX_{obs}, \sqrt{\sigma_f^2 + b^2\sigma_{obs}^2}\right) \quad (3)$$

The mean of the distribution is calculated by applying the observational constraint (X_{obs}) to the emergent linear inter-model relationship ($y = a + b*x$) of S_{seas} and S_{clm}. The standard deviation of the PDF distribution is estimated by ac-

counting for both observational uncertainty (σ_{obs}) and the prediction interval of the emergent relationship (σ_f).

The hereby constrained S_{clm} (here defined as $S_{\text{clm}*}$) is then used to estimate the constrained surface phytoplankton concentration change by the end of the 21st century ($R_{\text{sphy}*}$) by reordering Eq. (2) to $R_{\text{clm}*} = R_{\text{MLD}} * S_{\text{clm}*}$. The uncertainty in the post-constraint projection for the relative surface phytoplankton concentration variation is calculated by accounting for uncertainties from both the constrained long-term sensitivity ($\sigma_{S_{\text{clm}*}}$) and the MLD projection ($\sigma_{R_{\text{MLD}}}$) through error propagation:

$$\mathcal{N}\left(R_{\text{sphy}*},\ \sigma_{\text{sphy}*}\right) = \mathcal{N}\left(R_{\text{MLD}} \cdot S_{\text{clm}*},\ |R_{\text{MLD}} \cdot S_{\text{clm}*}|\right.$$
$$\left. \sqrt{\left(\frac{\sigma_{R_{\text{MLD}}}}{R_{\text{MLD}}}\right)^2 + \left(\frac{\sigma_{S_{\text{clm}*}}}{S_{\text{clm}*}}\right)^2}\right). \tag{4}$$

2.4 Observational constraints

The observation-based estimate of S_{seas} is based on monthly MLD data from the Argo mixed-layer database (http://mixedlayer.ucsd.edu/, last access: 26 October 2022) and satellite-derived monthly surface chlorophyll data from the merged satellite product GlobColour (https://www.globcolour.info/, last access: 13 October 2022) during the period 2000–2009. The observational MLD is calculated based on the temperature threshold estimate (threshold of 0.2 °C; Holte and Talley, 2009), consistent with the MLD diagnostic available from the MME. Surface chlorophyll is used as a reliable proxy for surface phytoplankton under the current climate, as it is a comparatively well-observed variable. Under the common assumption that all properties (except light) are considered homogeneous within the mixed layer (Westberry et al., 2008), we assume that phytoplankton concentrations across the mixed layer are well reflected by surface phytoplankton concentration. The seasonal variation in the observability of surface chlorophyll from satellite data is mainly affected by the winter light conditions and varying ice cover to the south of the research region. The impact of cloud cover in the research region is minor at a monthly temporal resolution (Fig. A4).

2.5 Trophic transfer efficiency

Given the simplicity of models and the limitations of their outputs, the trophic transfer efficiency (TTE; Eq. 5) is simply defined as the ratio of the total (depth-integrated) biomass of zooplankton to that of phytoplankton following Barnes et al. (2010):

$$\text{TTE} = \frac{\sum_{z=0}^{\text{zmax}} \text{zoo} \times \text{d}h}{\sum_{z=0}^{\text{zmax}} \text{phy} \times \text{d}h}, \tag{5}$$

where phy and zoo represent the phytoplankton and zooplankton biomass concentrations (unit: mg C m^{-3}), respectively; $\text{d}h$ indicates the thickness of each grid box; and zmax is the depth of the water column.

The dimensionless TTE reflects the biomass or energy transfer between trophic levels and is typically estimated based on the biomasses or productivities of trophic levels. We used biomass instead of productivity to quantify the TTE, as biomass can be directly compared to observations and is available from more models than productivity data (Table 1).

3 Results

3.1 Stable phytoplankton biomass in a changing climate: a shifting balance of bottom-up and top-down control in the Southern Ocean

The multi-model ensemble (MME) projects that the total phytoplankton biomass will remain relatively stable ($-2 \pm 8\%$) throughout the 21st century, following the SSP5-8.5 scenario (Fig. 4a). Future changes in the total phytoplankton biomass are largely determined by the competing effects of increasing primary production (bottom-up, Fig. 4b) and grazing by zooplankton (top-down, Fig. 4c). Understanding the complex interplay between bottom-up and top-down controls is crucial for projecting how phytoplankton will respond to future climate change.

Projected increases in the total primary production ($10 \pm 11\%$) show that phytoplankton growth conditions are improving with climate change, indicating weakening bottom-up control (Fig. 4b). On these centennial timescales, climate-change-induced changes in primary production in the subantarctic and subpolar Antarctic regions are tightly coupled to MLD-driven bottom-up changes (e.g., light, nutrients, and temperature) that also drive changes on observed contemporary seasonal timescales (Arteaga et al., 2020; Leung et al., 2015). As the MLD is projected to shoal by $12 \pm 5\%$ over the course of the 21st century (Fig. 5a), phytoplankton in the water column will largely stay closer to the surface, not being passively mixed down, thereby experiencing better light and temperature conditions. As a result, phytoplankton are projected to have a higher growth rate in the nutrient-replete Southern Ocean (dashed line in Fig. 4b).

Despite increasing total primary production, the total phytoplankton biomass remains relatively stable throughout the 21st century mainly because of enhanced zooplankton grazing ($14 \pm 15\%$) and thus intensified top-down control (Fig. 4c). With top-down control exhibiting an increasing trend similar to bottom-up condition under climate change, phytoplankton biomass stays in a dynamic balance despite the flux changes and thereby appears not to respond to the changing climate. An enhanced role of grazing under climate change is consistent with findings in Laufkötter et al. (2015).
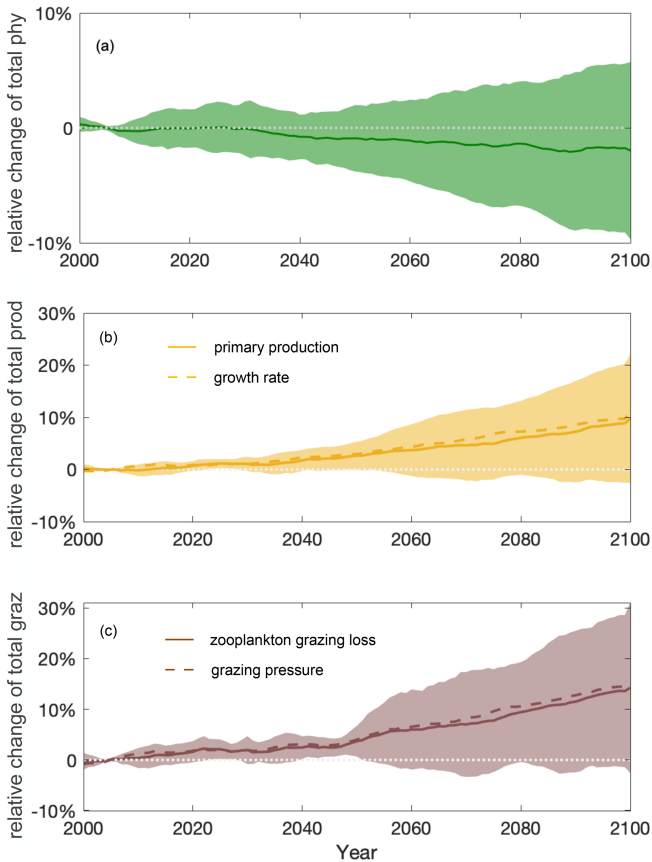
Figure 4. Stable total phytoplankton projections over the course of the 21st century due to a shifting balance of bottom-up and top-down control. Multi-model ensemble (MME) projections of the relative changes in total **(a)** phytoplankton (phy, dark green), **(b)** phytoplankton production (prod, yellow), and **(c)** grazing loss from zooplankton (graz, brown) from 2000 to 2100 under the SSP5-8.5 scenario, with shading indicating 1 standard deviation across the ESMs, relative to the respective mean values of the first decade of the 21st century (2000–2009) in the Southern Ocean. Solid lines indicate the multi-model mean. Dashed lines in **(b)** and **(c)** indicate the MME-averaged phytoplankton growth rate (estimated for individual models as integrated production divided by integrated biomass) and grazing pressure (estimated as integrated grazing loss divided by integrated biomass), respectively. The time series are filtered using a 10-year moving average.

3.2 Increasing surface phytoplankton concentration: intensified top-down control shifts trophic structure

The increasing top-down control and grazing pressure on phytoplankton may be a consequence of rising phytoplankton concentrations due to mixed-layer shoaling (Fig. 5a and b) and higher temperatures (Fig. A5) under climate change. Apart from total phytoplankton biomass, which reflects the total amount of food available to zooplankton, the concentration of phytoplankton is also a crucial factor in zooplankton grazing, as the feeding efficiency of zooplank-
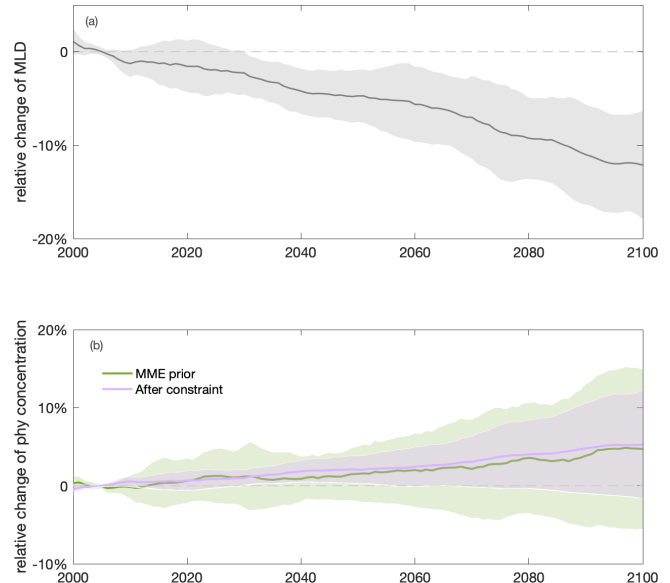

Figure 5. Shoaling of annual mean mixed-layer depth (MLD) and increasing annual mean surface phytoplankton concentration towards the end of the century in the Southern Ocean. Multi-model ensemble (MME) projections of changes in annual mean **(a)** MLD (grey) and **(b)** surface phytoplankton concentration (sphy) before (light green) and after (purple) applying the emergent constraint, from 2000 to 2100, relative to the mean values of the first decade of the 21st century (2000–2009), with shading indicating 1 standard deviation, under the SSP5-8.5 scenario. The time series are filtered using a 10-year moving average.

ton depends directly on the concentration of phytoplankton. Increasing phytoplankton concentration, due to shoaling mixed-layer depths, enhances encounter efficiency between zooplankton (the predator) and phytoplankton (the prey), enabling more efficient grazing (dashed line in Fig. 4c) and thus a stronger top-down control on phytoplankton. This mechanism is apparent in the correlation between mixed-layer depth and phytoplankton grazing loss due to zooplankton on the long-term timescale (Fig. A6) and has previously been found on a seasonal scale in present-day productive systems (Xue et al., 2022a). Additionally, higher temperatures are associated with increased zooplankton grazing rates and, thereby, a stronger top-down control on phytoplankton (Caron and Hutchins, 2013), though only a few CMIP6 models include temperature-dependent grazing (Rohr et al., 2023).

Increased top-down grazing pressure results in higher trophic transfer efficiency by the end of the century ($4 \pm 7\%$; Eq. 5, Fig. 6b). The rising trophic transfer efficiency indicates a potential change in trophic structure, with relatively more zooplankton and fewer phytoplankton in the future climate. In contrast to the projection of the slightly decreasing total phytoplankton biomass ($-2 \pm 8\%$), the total biomass of zooplankton, a phytoplankton predator, is projected to increase
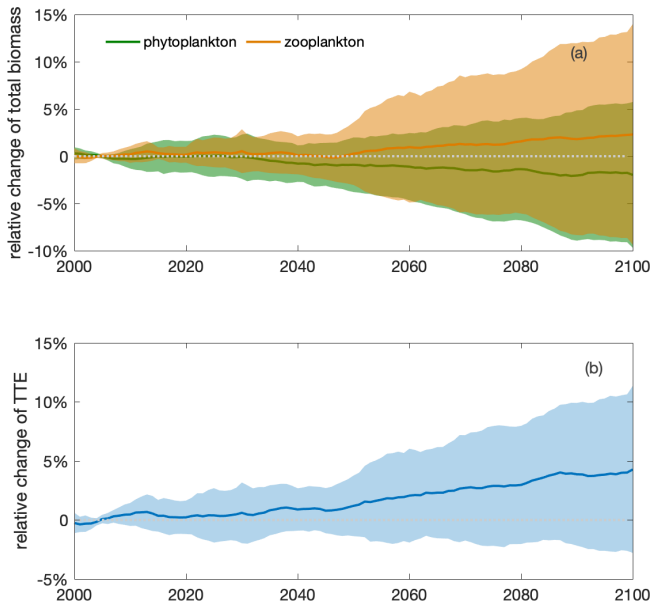
Figure 6. An increase in the total zooplankton biomass and trophic transfer efficiency (TTE) during the 21st century indicates intensified top-down control and a shift in trophic structure. Multi-model ensemble (MME) projections of the relative changes in **(a)** total (depth-integrated) phytoplankton (green) and zooplankton (orange) biomasses and **(b)** trophic transfer efficiency (blue; defined as the ratio of the two; see Eq. 5) from 2000 to 2100 under the SSP5-8.5 scenario, with shading indicating 1 standard deviation, relative to the respective mean values of the first decade of the 21st century (2000–2009) in the Southern Ocean. The time series are filtered using a 10-year moving average.

by 2 ($\pm$11) % under climate change (Fig. 6a). Zooplankton appear to be favoured by changing environmental conditions and food resources and are grazing down phytoplankton. The phenomenon of a positive change on a higher trophic level and a negative change on the lower trophic level indicates increasing top-down control of the lower trophic level by the higher one (Fig. 1 in Chust et al., 2014).

3.3 Constraining the increasing surface phytoplankton concentration: the underlying mechanism of intensified top-down control

3.3.1 Opposing trends of surface phytoplankton concentrations and mixed-layer depths on timescales of seasons and of climate change

As phytoplankton concentration is an indicator of grazing pressure, the large inter-model differences in projected changes from the 2000s to the 2090s (5 $\pm$ 10 %; Fig. 5b) cause a large number of the inter-model differences of projected changes in phytoplankton top-down control. Individual model-projected surface phytoplankton concentration changes range from −10 % to +32 % and in particular include zero and negative changes in the Southern Ocean by the

end of the century. The mechanisms previously suggested to explain the long-term changes in phytoplankton, such as light and temperature changes, are also responsible for their seasonal variability in the Southern Ocean (Leung et al., 2015; Henley et al., 2020).

Under the current climate, seasonalities of mixed-layer depths and surface chlorophyll concentration are anticorrelated in both observations and model simulations. The observed surface chlorophyll in the Southern Ocean exhibits a clear seasonal cycle, peaking in late austral spring and early austral summer (Fig. 7). This seasonal cycle of chlorophyll is opposite that of mixed-layer depth (MLD), with shallow MLD in austral summer coinciding with relatively high surface chlorophyll and deep MLD in austral winter coinciding with relatively low surface chlorophyll. Such an opposite relationship between surface chlorophyll and MLD on a seasonal scale has been previously shown in observations (Uchida et al., 2019; Arteaga et al., 2020) and model simulations (Song et al., 2018; Arteaga et al., 2020; Le Quéré et al., 2016). This relationship is thought to be mainly caused by the seasonal dilution of phytoplankton and by growth limitation along with zooplankton grazing. MLD reveals higher uncertainty compared to the extensively covered observed chlorophyll (satellite-based estimates), likely due to the scarcity of in situ-based data used to estimate the MLD. The individual models largely agree with the observed seasonal cycles, though with some spread (Fig. 7). Such a spread is not unexpected given the structural differences of the biogeochemical models that include varying considerations and representations of the chlorophyll-to-carbon (chl : C) ratio, grazing, and nutrient limitations (such as iron). On average, the modelled MLD maximum shows a lag of around a month compared to observational estimates, which is reflected in a similar lag in the chlorophyll seasonality. In both observations and models there is a lag between the timing of the peaks of minimum chlorophyll and maximum MLD in winter. This lag is likely due to poor light conditions in deep MLDs triggering an increase in the chl : C ratio, where increasing chlorophyll pigments mask a continued decrease in the phytoplankton biomass (organic carbon) concentration in deepening MLDs (Geider, 1987; Arteaga et al., 2016).

3.3.2 Using contemporary seasonality to constrain projections of surface phytoplankton concentration

Despite a good understanding of the top-down and bottom-up mechanisms in ESMs in the Southern Ocean, as explained above, the inter-model uncertainty in these mechanisms remains large. Therefore, we employ an emergent relationship between surface phytoplankton biomass and mixed-layer depth to reduce these uncertainties. A linear relationship ($r^2 = 0.65$, Fig. 8a) exists across the ESM ensemble between this sensitivity of chlorophyll to changes in MLD on a seasonal scale in the current climate (seasonal sensitiv-
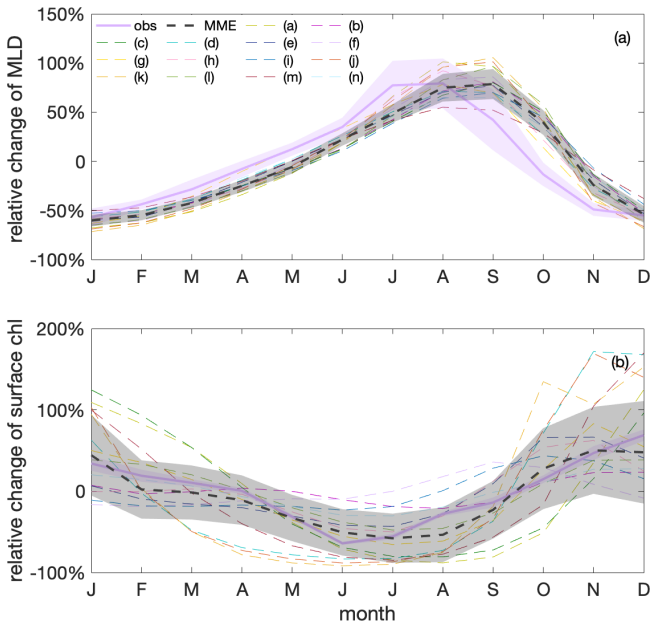
Figure 7. Surface chlorophyll (chl) concentration shows a clear seasonal cycle that is anticorrelated with mixed-layer depths (MLDs) in both observations and model simulations. Seasonal cycles of **(a)** MLD and **(b)** chl variations relative to their respective annual mean values, based on observations (GlobColour; purple) and a multi-model ensemble (MME; grey); the dashed black line marks the MME median value, and the shadings indicate the standard deviations of observations and the MME, respectively. Thin dashed differently coloured lines show individual models listed in Table 1 that contribute to the MME median value.

ity, S_{seas}; Eq. 1) and the sensitivity of surface phytoplankton to changes in MLD with climate change (climate change sensitivity, S_{clm}; Eq. 2), as expected based on previous studies (Leung et al., 2015; Henley et al., 2020). The relationship suggests that models within which surface chlorophyll is more sensitive to MLD changes on a seasonal scale also tend to show a larger sensitivity on a longer-term scale. Moreover, the slope of the emergent relationship is nearly 1. A one-to-one relationship indicates the same sensitivities of the leading mechanism on different timescales (Williamson et al., 2021). Though the sensitivities of chlorophyll to changes in MLD on a seasonal scale from individual models show some spread, it is important to note that the models deviating from the observed sensitivity are still considered capable of representing the relationship between chlorophyll sensitivity to MLD changes across seasonal and long-term scales. The correlation between mixed-layer depth and surface phytoplankton on a long-term climate scale is consistent with reduced dilution and a weakening of bottom-up controls, analogous to the most important mechanisms on seasonal scales: when the MLD is shoaling and phytoplankton are being contained in a shallower surface mixed layer with higher average light intensity and temperature, resulting in phytoplankton grow-

ing better and concentrations being expected to increase (Xue et al., 2022b). With this, we can use the relationship to constrain the projection of the surface phytoplankton concentration under climate change.

Applying the emergent constraint derived from the observations under current seasonality confirms the increasing trend of surface phytoplankton concentration by the end of the 21st century (Fig. 5b), thereby indicating intensified top-down control, with higher confidence. Utilising the observational constraint on the seasonal sensitivity (S_{seas}), the emergent constraint (Sect. 2.3) adjusts the estimate of the long-term sensitivity (S_{clm}) from -0.38 (± 0.69) to -0.44 (± 0.46) (Fig. 8b). Thus, the surface phytoplankton concentration becomes slightly more sensitive to MLD shoaling than previously suggested by the unconstrained MME results. In combination with the MME-projected MLD change, our emergent constraint implies a 5 (± 7) % (unconstrained: 5 ± 10 %) increase in surface phytoplankton concentrations in the Southern Ocean by the end of the 21st century (Eq. 4). The emergent constraint reduces the uncertainty in the surface phytoplankton projection by 34 % (Fig. 5b). Based on the constraint, the possibility of a surface phytoplankton concentration decrease becomes less likely (16 %) compared to what was expected based on the MME alone (29 %). Our results therefore suggest, with enhanced confidence, an increase in surface phytoplankton concentration in the subantarctic and subpolar Antarctic regions of the Southern Ocean by the end of the century (Fig. 5). This projection of increasing surface phytoplankton concentration, alongside rising temperatures (Fig. A5), suggests an increased likelihood of enhanced grazing pressure and thus more intensified top-down control under climate change.

4 Discussion

4.1 Phytoplankton under climate change

In this study, we have delved into the complex interplay of bottom-up and top-down mechanisms affecting phytoplankton dynamics in the Southern Ocean under climate change. Building on the understanding of these mechanisms across current seasonal and future climate change scales, we employ emergent constraints to refine surface phytoplankton projection and emphasise weakening bottom-up control and the growing importance of top-down control. This approach not only advances our understanding of the Southern Ocean's ecosystem response to climate change but also illustrates the potential for similar applications in other productive oceanic regions with notable model uncertainties, such as coastal upwelling regions (Chang et al., 2023).

While emergent constraints enable the MME to project future phytoplankton changes with higher confidence, the often too simplistic representation of the iron cycle in ESMs (Tagliabue et al., 2017) may hide additional uncertainties and
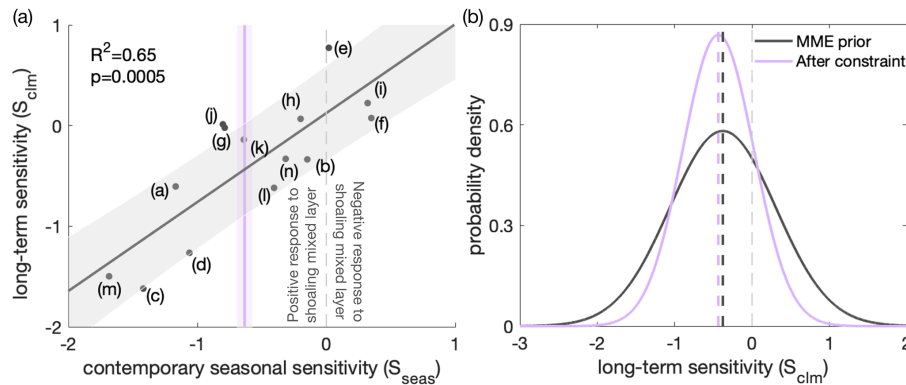
Figure 8. Application of an emergent constraint to the long-term sensitivity (S_{clm}) of surface phytoplankton concentration to mixed-layer depth (MLD), based on the contemporary seasonal sensitivity (S_{seas}) of surface chlorophyll concentration to MLD. **(a)** Long-term sensitivity (S_{clm}; Eq. 2) under climate change against contemporary seasonal sensitivity (S_{seas}; Eq. 1) of the relative change in the surface chlorophyll (for S_{seas}) or phytoplankton (for S_{clm}) concentration to MLD for the multi-model ensemble (MME; black dots, corresponding to the models listed in Table 1). The fit of a linear regression (black line) and the associated 68 % prediction intervals are shown as a black line and grey shading, respectively. The vertical purple line indicates an observational constraint, with purple shading indicating the associated uncertainty, calculated as the standard error in the climatological S_{seas} of the observed time series (Fig. 3). The dashed light-grey line separates the positive (to the left) and negative (to the right) responses across models of surface chlorophyll to MLD shoaling under present-day seasonality. **(b)** Probability density functions (PDFs) of S_{clm}. The black line shows the "MME prior" PDF, assuming all model projections are equally likely and come from a Gaussian distribution. The purple line shows the observationally constrained PDF (it has a similar mean but is narrower). Dashed lines indicate the mean values of the future climate sensitivity before (black) and after (purple) applying the constraint.

the oversimplified food web formulations potentially limit the reproducibility of phytoplankton composition changes, underscoring the need for model improvements to capture these critical changes and understand future ecosystem dynamics comprehensively (Petrou et al., 2016; Krumhardt et al., 2022). In addition to impacts from light and temperature change, the micronutrient iron is often deemed limiting in the Southern Ocean, which affects phytoplankton growth and limits the magnitude of phytoplankton blooms (Martin et al., 1990; Moore et al., 2013; Arteaga et al., 2020). Over recent decades, an increase in iron stress has been observed in the Southern Ocean due to changing mixed-layer dynamics (Ryan-Keogh et al., 2023). However, with the progression of climate change, an increase in the atmospheric iron supply, a crucial source for the Southern Ocean, is projected to rise through various sources (IPCC, 2019; Hamilton et al., 2020). For instance, the deposition of soluble iron is expected to increase due to more frequent and intense wildfires (Bowman et al., 2020), along with increasing wind and desertification (Woodward et al., 2005). Despite its importance to phytoplankton growth in the Southern Ocean, the processes of producing and cycling iron are still not yet fully understood, and it was not until the early 2000s that global ocean models began incorporating iron (Tagliabue et al., 2017; Moore et al., 2001). Even in the MME used here from the most recent generation of Earth system models, 3 out of 14 ESMs do not represent the iron cycle at all (Table 1). Of the 11 ESMs that include the iron cycle, only 9 models provide output on iron, simulating varying changes in iron availability in the South-

ern Ocean. However, across the multi-model mean, there is no discernible trend in surface iron concentration (Fig. A7). As a result, models with or without iron limitation do not reveal clear differences in the projection of phytoplankton responses to climate change (Fig. A8), though models with iron representation show a much larger spread than those without. Given the very different representation of the iron cycle in current ESMs and the complex interplay between iron and its biological responses, along with the multitude of external processes affecting its availability, projecting changes in iron availability likely adds a large uncertainty to phytoplankton projections under climate change (Petrou et al., 2016).

4.2 Enhancing understanding of top-down processes under climate change

While bottom-up mechanisms are well recognised and studied (Deppeler and Davidson, 2017; Frenger et al., 2018; Arteaga et al., 2020; Leung et al., 2015), the impact of top-down effects on phytoplankton has been less emphasised, largely due to insufficient observational data. Despite significant advancements in ocean ecosystem monitoring over recent decades, such as the COPEPOD dataset (Coastal & Oceanic Plankton Ecology, Production, & Observation Database; https://www.st.nmfs.noaa.gov/copepod/, last access: 25 June 2021; Moriarty and O'brien, 2013), supporting advanced relevant studies, a notable gap persists in observational data that specifically target higher trophic levels and data coverage in the Southern Ocean. This gap underscores the need for a more comprehensive observational sys-

tem, especially concerning quantities, such as zooplankton biomass, community composition, and traits, to enhance the robustness of projections of future plankton dynamics and trophic transfer (Prowe et al., 2022). It is important to understand zooplankton physiology to identify and further constrain the relevant key parameters, such as prey preferences, maximum ingestion rates, and zooplankton temperature sensitivity (Prowe et al., 2019; Petrik et al., 2022).

Climate change projections of top-down variables are highly uncertain (Laufkötter et al., 2015; Lotze et al., 2019; Kwiatkowski et al., 2020; Rohr et al., 2023), mainly because zooplankton and food web formulations in large-scale models are oversimplified, posing a substantial caveat. The formulation of zooplankton in numerical models is crucial in regulating the mortality of modelled phytoplankton, which in turn has a significant impact on planktonic dynamics (Le Quéré et al., 2016; Prowe et al., 2019). Top-down grazing by zooplankton is influenced by factors including traits of both the prey and predator; the prey concentration; and also the type of predator–prey relationship used in a model, such as the different Holling types (Kiørboe, 2009; Xue et al., 2022a; Anderson et al., 2010). In addition, the lack of observations has hindered the calibration of most global biogeochemical models to accurately represent top-down controls (Stock et al., 2014b). To improve the top-down projection, ocean biogeochemical models should more regularly save zooplankton-related variables as standard model output to allow for comprehensive analyses (Laufkötter et al., 2015; Le Grix et al., 2022). Such zooplankton-related variables should include not only bulk variables such as biomass but also fluxes in order to better track the energy flux through the ecosystem. Overall, model representations of phytoplankton will benefit from a more extensive assessment of zooplankton through a more accurate simulation of the top-down process.

4.3 Differences in trends of biomass and production

The divergent trends in the total phytoplankton biomass and production under climate change demonstrated in our study are attributed to the increasing importance of top-down control. Here, we show that total phytoplankton biomass remains relatively stable in the Southern Ocean, while total phytoplankton production continues to increase. Previous investigations of the phytoplankton response to climate change focusing on biomass (Marinov et al., 2010; Kwiatkowski et al., 2019; Lotze et al., 2019) versus production (Behrenfeld et al., 2006; Laufkötter et al., 2015; Deppeler and Davidson, 2017; Kwiatkowski et al., 2020) tended to conclude that changes would be of the same sign for the two variables, with a negative response in low-latitude regions due to increasing nutrient limitations and a positive response in high-latitude regions as a result of improving light conditions. Further investigations into the trophodynamics using biomass (Chust et al., 2014; Kwiatkowski et al., 2019) and production (Stock et al., 2014a) have also demonstrated con-

sistent findings, with low-latitude regions exhibiting negative trophic amplification (with decreases in higher trophic levels exceeding those in lower trophic levels) and high-latitude regions demonstrating positive trophic amplification (with increases in higher trophic levels exceeding those in lower trophic levels) under climate change. The change in biomass is determined by the competing effects of bottom-up (production) and top-down (loss) processes. Projections using biomass and production tend to yield the same trends when top-down processes are negligible or play a secondary role in comparison with bottom-up processes. However, when top-down processes are of a similar magnitude (e.g., Fig. 4) or even more important than bottom-up processes, projections using biomass and production may yield different results as biomass and production represent two distinct ways of viewing and understanding the ecosystem. While biomass focuses on the standing stock that can be measured, production quantifies the energy flow among different components of the ecosystem. Our finding of different trends in phytoplankton biomass and production under global warming underscores the increasing importance of top-down processes in the future Southern Ocean ecosystem.

5 Conclusions

In this study, we present the future phytoplankton response to climate change under a high-emission, no-mitigation (SSP5-8.5) scenario in the subantarctic and subpolar Antarctic regions (40–60° S) of the Southern Ocean using a multi-model ensemble. We find that the total phytoplankton biomass stays relatively stable over the course of the 21st century as a result of a dynamic balance between bottom-up and top-down control. Future phytoplankton growth conditions are expected to improve as a result of the shoaling mixed layer and increasing temperature, thereby weakening bottom-up control, consistent with previous studies. Meanwhile, the shoaling mixed layer will further concentrate the phytoplankton biomass and make phytoplankton more accessible to zooplankton, thereby intensifying grazing pressure and hence top-down control. The continuously growing negative effect of increasing top-down control compensates for the positive effects of improving bottom-up conditions, resulting in a well-balanced flux budget that keeps the total phytoplankton biomass stable under climate change.

We further employ the approach of an emergent constraint to increase our confidence in the increasing trend of surface phytoplankton concentration, which could be the underlying mechanism that contributes to the intensifying top-down processes under climate change. For that, we make use of the observed relationship between seasonal variations in mixed-layer depth and surface chlorophyll concentration. The relationship originates from the combined effects of bottom-up and top-down processes as well as physical dilution caused by mixing across the varying mixed layers. The application

of the observational constraint to a climate projection under the SSP5-8.5 scenario confirms the increasing trend of surface phytoplankton concentration and reduces the uncertainty in its future projections by more than a third. This further promotes confidence in intensified top-down control in the changing climate.

This study highlights the need to understand the balance of bottom-up versus top-down control of phytoplankton. In particular, mechanisms promoting a dominance of top-down control, which are of growing importance for climate change, have been understudied. Top-down control is typically treated as a mere "closure term" in biogeochemical models for climate research, such as CMIP models, which prioritise numerical stability while often neglecting zooplankton physiology and adaptive capacities. We argue that zooplankton physiology and adaptive capacities are crucial for accurately simulating phytoplankton dynamics. To improve our understanding of the response of phytoplankton to climate change, there is a pressing need for dedicated observational and modelling efforts. Such efforts include but are not limited to long-term and continuous observational time series of phytoplankton and zooplankton biomass and traits to enhance our understanding of the response of feeding processes to changing environmental conditions. Such observations, in turn, will facilitate improved top-down formulations in models. Further, our results suggest that previous studies (e.g. Chust et al., 2014; Kwiatkowski et al., 2017; Stock et al., 2014a) that result in the same conclusion for phytoplankton biomass and production imply a negligible or secondary role of top-down processes. With the increasing importance of top-down processes under climate change, phytoplankton biomass and production could display divergent trends, as shown in our results. Our results demonstrate that total phytoplankton biomass in the Southern Ocean can remain stable despite increasing phytoplankton production as a result of a shifting balance from bottom-up towards enhanced top-down control.

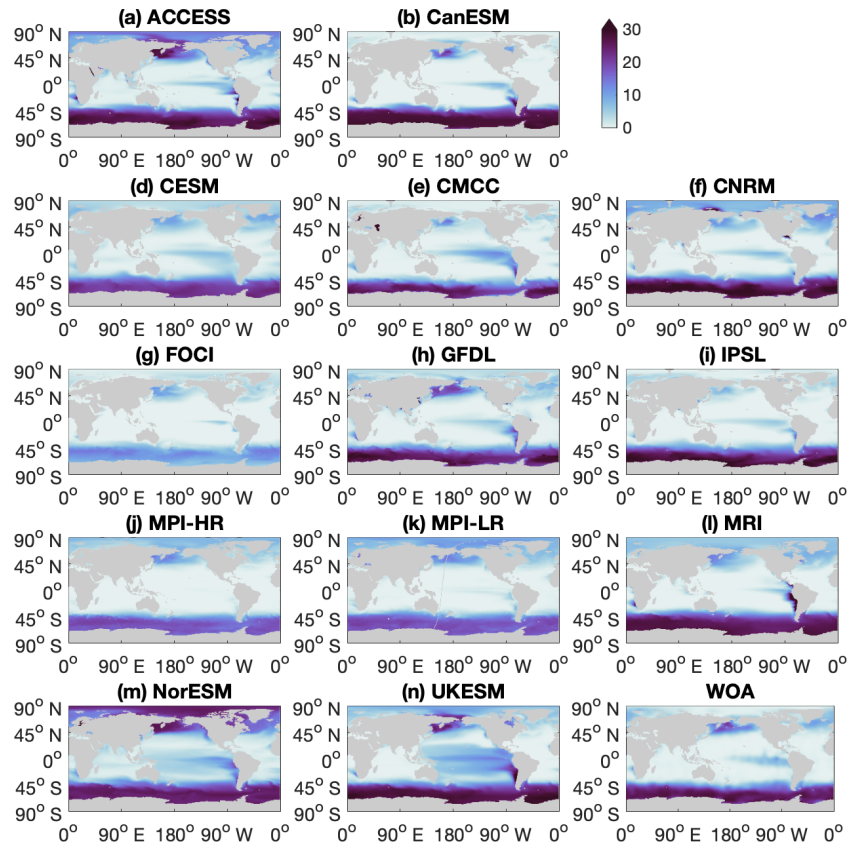## Appendix A: Additional figures

Figure A1. Maps for individual climate models and observational data from the World Ocean Atlas (WOA), showing annual mean surface nitrate concentration (unit: mmol m^{-3}) in the contemporary climate (2000–2009).
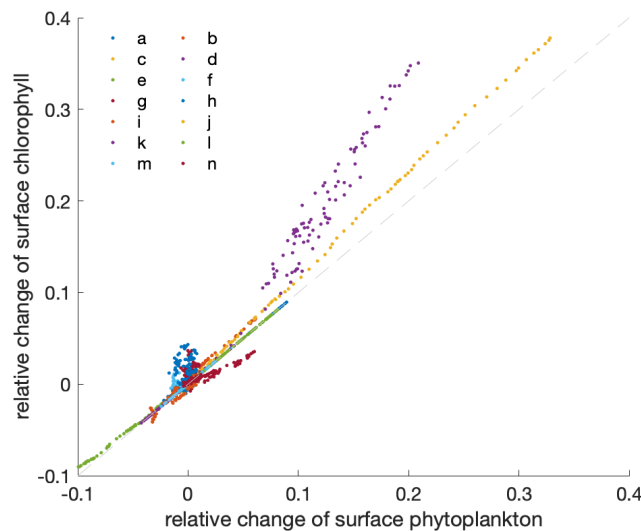

Figure A2. Relation between the relative changes in the annual mean surface phytoplankton concentration and surface chlorophyll concentration. The dashed light-grey line indicates the 1 : 1 line. Differently coloured dots indicate individual models as listed in Table 1 in the main paper, with individual dots representing consecutive years for the time period 2000 to 2100.
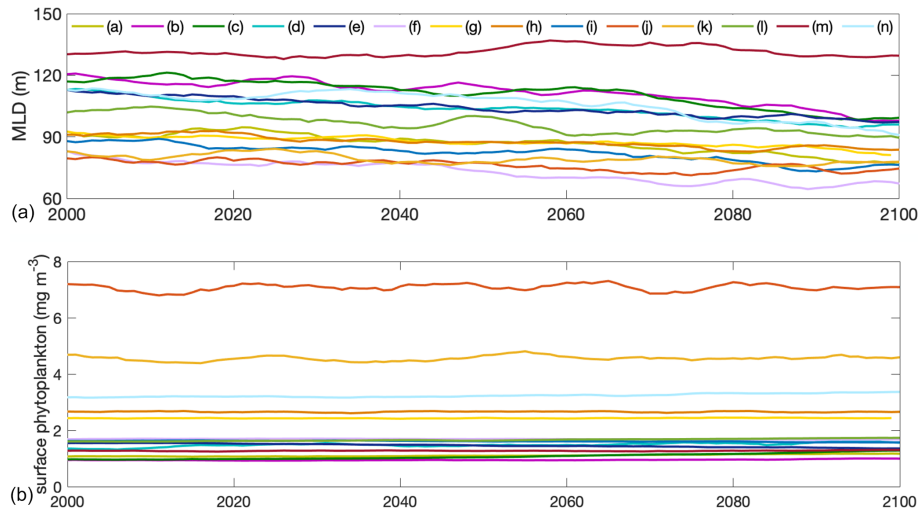
Figure A3. Projections of **(a)** mixed-layer depth and **(b)** surface phytoplankton concentration in absolute values from 2000 to 2100 of individual models of the multi-model ensemble in the Southern Ocean. Differently coloured lines show individual models listed in Table 1 of the main paper.
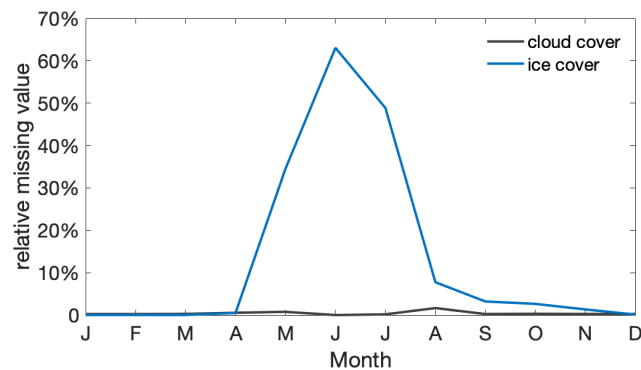
Figure A4. Seasonal cycle of the average portion of satellite chlorophyll missing per month and per grid box within the research area due to cloud cover (black) and ice cover or no light (blue).
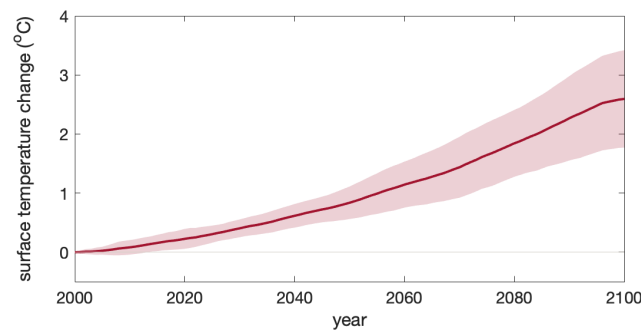
Figure A5. Increasing sea surface temperature under climate change in the Southern Ocean. Multi-model ensemble (MME) projections of the sea surface temperature change (unit: °C) from 2000 to 2100 under the SSP5-8.5 scenario, with shading indicating 1 standard deviation. The time series are filtered using a 10-year moving average.
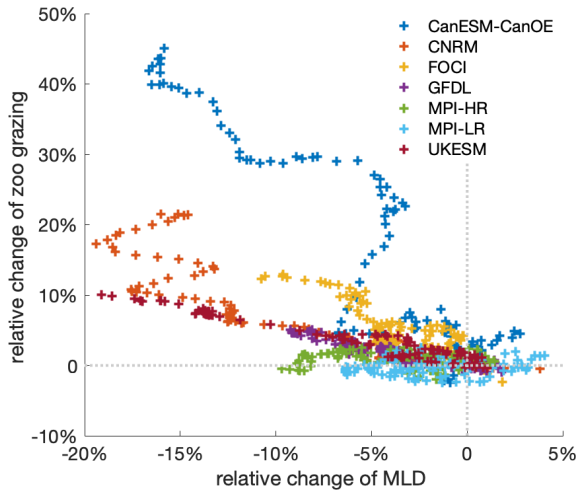
Figure A6. Mixed-layer depth directly influences zooplankton grazing by affecting phytoplankton biomass concentration, which alters prey–predator encounters. Relation between relative anomalies of annual mean mixed-layer depth and zooplankton grazing from 2000 to 2100 under the SSP5-8.5 scenario, relative to the mean values of the first decade of the 21st century (2000–2009) in the Southern Ocean. The time series are filtered using a 10-year moving average; different colours denote different climate models. Note that not all models include grazing as an output variable, which is why the number of models here is smaller.
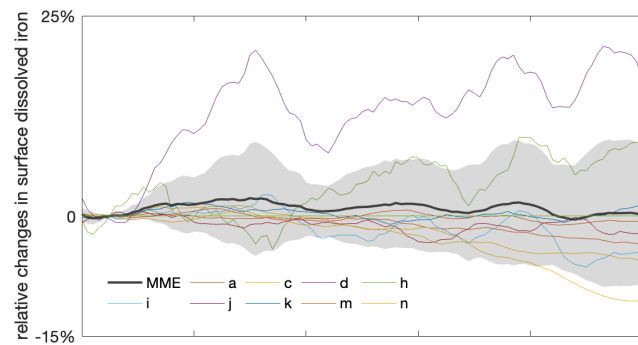

Figure A7. Varying projected changes in future surface dissolved iron in the Southern Ocean. Multi-model ensemble (MME) projections of the relative changes in dissolved iron from 2000 to 2100 under the SSP5-8.5 scenario, with shading indicating 1 standard deviation, relative to the respective mean values of the first decade of the 21st century (2000–2009). Dissolved iron data are only available from a limited number of models. The letter in the legend indicates the respective model listed in Table 1. The time series are filtered using a 10-year moving average.

Figure A8. ESMs that include or do not include iron limitation project the total phytoplankton change similarly, albeit with a larger spread if iron is simulated. Beeswarm plot of the relative changes in the total phytoplankton biomass over the 21st century under the SSP5-8.5 scenario using models that explicitly include iron limitation (red) and no iron limitation (blue).

Author contributions. TX and IF designed the study. TX conducted the analysis with support from IF and JT. TX wrote the first draft of the manuscript and produced all figures and tables. All authors discussed the results and contributed to the final writing of the manuscript.

Competing interests. The authors declare that they have no conflict of interest.

Disclaimer. Publisher's note: Copernicus Publications remains neutral with regard to jurisdictional claims made in the text, published maps, institutional affiliations, or any other geographical representation in this paper. While Copernicus Publications makes every effort to include appropriate place names, the final responsibility lies with the authors.

Code availability. This study did not involve the development of new model codes. The analysis codes are available from the corresponding author upon request.

References

Anderson, T. R., Gentleman, W. C., and Sinha, B.: Influence of grazing formulations on the emergent properties of a complex ecosystem model in a global ocean general circulation model, Prog. Oceanogr., 87, 201–213, https://doi.org/10.1016/j.pocean.2010.06.003, 2010.

Arteaga, L. A., Pahlow, M., and Oschlies, A.: Modeled Chl: C ratio and derived estimates of phytoplankton carbon biomass and its contribution to total particulate organic carbon in the global surface ocean, Global Biogeochem. Cy., 30, 1791–1810, https://doi.org/10.1002/2016GB005458, 2016.

Arteaga, L. A., Boss, E., Behrenfeld, M. J., Westberry, T. K., and Sarmiento, J. L.: Seasonal modulation of phytoplankton biomass in the Southern Ocean, Nat. Commun., 11, 1–10, https://doi.org/10.1038/s41467-020-19157-2, 2020.

Barnes, C., Maxwell, D., Reuman, D. C., and Jennings, S.: Global patterns in predator–prey size relationships reveal size dependency of trophic transfer efficiency, Ecology, 91, 222–232, https://doi.org/10.1890/08-2061.1, 2010.

Behrenfeld, M. J., O'Malley, R. T., Siegel, D. A., McClain, C. R., Sarmiento, J. L., Feldman, G. C., Milligan, A. J., Falkowski, P. G., Letelier, R. M., and Boss, E. S.: Climate-driven trends in contemporary ocean productivity, Nature, 444, 752–755, https://doi.org/10.1038/nature05317, 2006.

Bopp, L., Monfray, P., Aumont, O., Dufresne, J.-L., Le Treut, H., Madec, G., Terray, L., and Orr, J. C.: Potential impact of climate change on marine export production, Global Biogeochem. Cy., 15, 81–99, https://doi.org/10.1029/1999GB001256, 2001.

Bopp, L., Aumont, O., Cadule, P., Alvain, S., and Gehlen, M.: Response of diatoms distribution to global warming and potential

implications: A global model study, Geophys. Res. Lett., 32, L19606, https://doi.org/10.1029/2005GL023653, 2005.

Bopp, L., Resplandy, L., Orr, J. C., Doney, S. C., Dunne, J. P., Gehlen, M., Halloran, P., Heinze, C., Ilyina, T., Séférian, R., Tjiputra, J., and Vichi, M.: Multiple stressors of ocean ecosystems in the 21st century: projections with CMIP5 models, Biogeosciences, 10, 6225–6245, https://doi.org/10.5194/bg-10-6225-2013, 2013.

Boucher, O., Servonnat, J., Albright, A. L., Aumont, O., Balkanski, Y., Bastrikov, V., Bekki, S., Bonnet, R., Bony, S., Bopp, L., and Vuichard, N.: Presentation and evaluation of the IPSL-CM6A-LR climate model, J. Adv. Model. Earth Sy., 12, e2019MS002010, https://doi.org/10.1029/2019MS002010, 2020.

Bowman, D. M., Kolden, C. A., Abatzoglou, J. T., Johnston, F. H., van der Werf, G. R., and Flannigan, M.: Vegetation fires in the Anthropocene, Nat. Rev. Earth Environ., 1, 500–515, https://doi.org/10.1038/s43017-020-0085-3, 2020.

Boyce, D. G., Lewis, M. R., and Worm, B.: Global phytoplankton decline over the past century, Nature, 466, 591–596, https://doi.org/10.1038/nature09268, 2010.

Caron, D. A. and Hutchins, D. A.: The effects of changing climate on microzooplankton grazing and community structure: drivers, predictions and knowledge gaps, J. Plankton Res., 35, 235–252, https://doi.org/10.1093/plankt/fbs091, 2013.

Chang, P., Xu, G., Kurian, J., Small, R. J., Danabasoglu, G., Yeager, S., Castruccio, F., Zhang, Q., Rosenbloom, N., and Chapman, P.: Uncertain future of sustainable fisheries environment in eastern boundary upwelling zones under climate change, Commun. Earth Environ., 4, 19, https://doi.org/10.1038/s43247-023-00681-0, 2023.

Chien, C.-T., Durgadoo, J. V., Ehlert, D., Frenger, I., Keller, D. P., Koeve, W., Kriest, I., Landolfi, A., Patara, L., Wahl, S., and Oschlies, A.: FOCI-MOPS v1 – integration of marine biogeochemistry within the Flexible Ocean and Climate Infrastructure version 1 (FOCI 1) Earth system model, Geosci. Model Dev., 15, 5987–6024, https://doi.org/10.5194/gmd-15-5987-2022, 2022.

Christian, J. R., Denman, K. L., Hayashida, H., Holdsworth, A. M., Lee, W. G., Riche, O. G. J., Shao, A. E., Steiner, N., and Swart, N. C.: Ocean biogeochemistry in the Canadian Earth System Model version 5.0.3: CanESM5 and CanESM5-CanOE, Geosci. Model Dev., 15, 4393–4424, https://doi.org/10.5194/gmd-15-4393-2022, 2022.

Chust, G., Allen, J. I., Bopp, L., Schrum, C., Holt, J., Tsiaras, K., Zavatarelli, M., Chifflet, M., Cannaby, H., Dadou, I., and Irigoien, X.: Biomass changes and trophic amplification of plankton in a warmer ocean, Glob. Change Biol., 20, 2124–2139, https://doi.org/10.1111/gcb.12562, 2014.

Danabasoglu, G., Lamarque, J.-F., Bacmeister, J., Bailey, D., DuVivier, A., Edwards, J., Emmons, L., Fasullo, J., Garcia, R., Gettelman, A., and Strand, W.: The community earth system model version 2 (CESM2), J. Adv. Model. Earth Sy., 12, e2019MS001916, https://doi.org/10.1029/2019MS001916, 2020.

Deppeler, S. L. and Davidson, A. T.: Southern Ocean phytoplankton in a changing climate, Front. Mar. Sci., 4, 40, https://doi.org/10.3389/fmars.2017.00040, 2017.

Dunne, J., Horowitz, L., Adcroft, A., Ginoux, P., Held, I., John, J., Krasting, J., Malyshev, S., Naik, V., Paulot, F., and Zhao,

M.: The GFDL Earth System Model version 4.1 (GFDL-ESM 4.1): Overall coupled model description and simulation characteristics, J. Adv. Model. Earth Sy., 12, e2019MS002015, https://doi.org/10.1029/2019MS002015, 2020.

ESA: GlobColour Project, https://www.globcolour.info/, last access: 22 May 2024.

ESGF: DKRZ ESGF-CoG Node, https://esgf-data.dkrz.de, last access: 22 May 2024.

Field, C. B., Behrenfeld, M. J., Randerson, J. T., and Falkowski, P.: Primary production of the biosphere: integrating terrestrial and oceanic components, Science, 281, 237–240, https://doi.org/10.1126/science.281.5374.237, 1998.

Frenger, I., Münnich, M., and Gruber, N.: Imprint of Southern Ocean mesoscale eddies on chlorophyll, Biogeosciences, 15, 4781–4798, https://doi.org/10.5194/bg-15-4781-2018, 2018.

Frölicher, T. L., Rodgers, K. B., Stock, C. A., and Cheung, W. W.: Sources of uncertainties in 21st century projections of potential ocean ecosystem stressors, Global Biogeochem. Cy., 30, 1224–1243, https://doi.org/10.1002/2015GB005338, 2016.

Geider, R. J.: Light and temperature dependence of the carbon to chlorophyll a ratio in microalgae and cyanobacteria: implications for physiology and growth of phytoplankton, New Phytol., 106, 1–34, https://doi.org/10.1111/j.1469-8137.1987.tb04788.x, 1987.

Hall, A., Cox, P., Huntingford, C., and Klein, S.: Progressing emergent constraints on future climate change, Nat. Clim. Change, 9, 269–278, https://doi.org/10.1038/s41558-019-0436-6, 2019.

Hamilton, D. S., Moore, J. K., Arneth, A., Bond, T. C., Carslaw, K. S., Hantson, S., Ito, A., Kaplan, J. O., Lindsay, K., Nieradzik, L., and Mahowald, N. M.: Impact of changes to the atmospheric soluble iron deposition flux on ocean biogeochemical cycles in the Anthropocene, Global Biogeochem. Cy., 34, e2019GB006448, https://doi.org/10.1029/2019GB006448, 2020.

Henley, S. F., Cavan, E. L., Fawcett, S. E., Kerr, R., Monteiro, T., Sherrell, R. M., Bowie, A. R., Boyd, P. W., Barnes, D. K., Schloss, I. R., and Shantelle, S.: Changing biogeochemistry of the Southern Ocean and its ecosystem implications, Front. Mar. Sci., 7, 581, https://doi.org/10.3389/fmars.2020.00581, 2020.

Holte, J. and Talley, L.: A new algorithm for finding mixed layer depths with applications to Argo data and Subantarctic Mode Water formation, J. Atmos. Ocean. Tech., 26, 1920–1939, https://doi.org/10.1175/2009JTECHO543.1, 2009.

Holte, J., Talley, L. D., Gilson, J., and Roemmich, D.: An Argo mixed layer climatology and database, Geophys. Res. Lett., 44, 5618–5626, https://doi.org/10.1002/2017GL073426, 2017 (data available at: http://mixedlayer.ucsd.edu/, last access: 22 May 2024).

IPCC: IPCC Special Report on the Ocean and Cryosphere in a Changing Climate, edited by: Pörtner, H.-O., Roberts, D. C., Masson-Delmotte, V., Zhai, P., Tignor, M., Poloczanska, E., Mintenbeck, K., Alegría, A., Nicolai, M., Okem, A., Petzold, J., Rama, B., and Weyer, N. M., Cambridge University Press, Cambridge, UK and New York, NY, USA, 755 pp., https://doi.org/10.1017/9781009157964, 2019.

Kessler, A. and Tjiputra, J.: The Southern Ocean as a constraint to reduce uncertainty in future ocean carbon sinks, Earth Syst. Dynam., 7, 295–312, https://doi.org/10.5194/esd-7-295-2016, 2016.

Kiørboe, T.: A mechanistic approach to plankton ecology, ASLO Web Lectures, 1, 1–91, 2009.

Krumhardt, K. M., Long, M. C., Sylvester, Z. T., and Petrik, C. M.: Climate drivers of Southern Ocean phytoplankton community composition and potential impacts on higher trophic levels, Front. Mar. Sci., 9, 916140, https://doi.org/10.3389/fmars.2022.916140, 2022.

Kwiatkowski, L., Bopp, L., Aumont, O., Ciais, P., Cox, P. M., Laufkötter, C., Li, Y., and Séférian, R.: Emergent constraints on projections of declining primary production in the tropical oceans, Nat. Clim. Change, 7, 355–358, https://doi.org/10.1038/nclimate3265, 2017.

Kwiatkowski, L., Aumont, O., and Bopp, L.: Consistent trophic amplification of marine biomass declines under climate change, Glob. Change Biol., 25, 218–229, https://doi.org/10.1111/gcb.14468, 2019.

Kwiatkowski, L., Torres, O., Bopp, L., Aumont, O., Chamberlain, M., Christian, J. R., Dunne, J. P., Gehlen, M., Ilyina, T., John, J. G., Lenton, A., Li, H., Lovenduski, N. S., Orr, J. C., Palmieri, J., Santana-Falcón, Y., Schwinger, J., Séférian, R., Stock, C. A., Tagliabue, A., Takano, Y., Tjiputra, J., Toyama, K., Tsujino, H., Watanabe, M., Yamamoto, A., Yool, A., and Ziehn, T.: Twenty-first century ocean warming, acidification, deoxygenation, and upper-ocean nutrient and primary production decline from CMIP6 model projections, Biogeosciences, 17, 3439–3470, https://doi.org/10.5194/bg-17-3439-2020, 2020.

Laufkötter, C., Vogt, M., Gruber, N., Aita-Noguchi, M., Aumont, O., Bopp, L., Buitenhuis, E., Doney, S. C., Dunne, J., Hashioka, T., Hauck, J., Hirata, T., John, J., Le Quéré, C., Lima, I. D., Nakano, H., Seferian, R., Totterdell, I., Vichi, M., and Völker, C.: Drivers and uncertainties of future global marine primary production in marine ecosystem models, Biogeosciences, 12, 6955–6984, https://doi.org/10.5194/bg-12-6955-2015, 2015.

Le Grix, N., Zscheischler, J., Rodgers, K. B., Yamaguchi, R., and Frölicher, T. L.: Hotspots and drivers of compound marine heatwaves and low net primary production extremes, Biogeosciences, 19, 5807–5835, https://doi.org/10.5194/bg-19-5807-2022, 2022.

Le Quéré, C., Buitenhuis, E. T., Moriarty, R., Alvain, S., Aumont, O., Bopp, L., Chollet, S., Enright, C., Franklin, D. J., Geider, R. J., Harrison, S. P., Hirst, A. G., Larsen, S., Legendre, L., Platt, T., Prentice, I. C., Rivkin, R. B., Sailley, S., Sathyendranath, S., Stephens, N., Vogt, M., and Vallina, S. M.: Role of zooplankton dynamics for Southern Ocean phytoplankton biomass and global biogeochemical cycles, Biogeosciences, 13, 4111–4133, https://doi.org/10.5194/bg-13-4111-2016, 2016.

Leung, S., Cabré, A., and Marinov, I.: A latitudinally banded phytoplankton response to 21st century climate change in the Southern Ocean across the CMIP5 model suite, Biogeosciences, 12, 5715–5734, https://doi.org/10.5194/bg-12-5715-2015, 2015.

Lotze, H. K., Tittensor, D. P., Bryndum-Buchholz, A., Eddy, T. D., Cheung, W. W., Galbraith, E. D., Barange, M., Barrier, N., Bianchi, D., Blanchard, J. L., and Worm, B.: Global ensemble projections reveal trophic amplification of ocean biomass declines with climate change, P. Natl. Acad. Sci. USA, 116, 12907–12912, https://doi.org/10.1073/pnas.1900194116, 2019.

Lovato, T., Peano, D., Butenschön, M., Materia, S., Iovino, D., Scoccimarro, E., Fogli, P., Cherchi, A., Bellucci, A., Gualdi, S., and Masina, S.: CMIP6 Simulations With the CMCC Earth System Model (CMCC-ESM2), J. Adv. Model. Earth Sy.,

14, e2021MS002814, https://doi.org/10.1029/2021MS002814, 2022.

Marinov, I., Gnanadesikan, A., Toggweiler, J., and Sarmiento, J. L.: The Southern Ocean biogeochemical divide, Nature, 441, 964–967, https://doi.org/10.1038/nature04883, 2006.

Marinov, I., Doney, S. C., and Lima, I. D.: Response of ocean phytoplankton community structure to climate change over the 21st century: partitioning the effects of nutrients, temperature and light, Biogeosciences, 7, 3941–3959, https://doi.org/10.5194/bg-7-3941-2010, 2010.

Martin, J. H., Gordon, R. M., and Fitzwater, S. E.: Iron in Antarctic waters, Nature, 345, 156–158, https://doi.org/10.1038/345156a0, 1990.

Mauritsen, T., Bader, J., Becker, T., Behrens, J., Bittner, M., Brokopf, R., Brovkin, V., Claussen, M., Crueger, T., Esch, M., and Roeckner, E.: Developments in the MPI-M Earth System Model version 1.2 (MPI-ESM1. 2) and its response to increasing CO_2, J. Adv. Model. Earth Sy., 11, 998–1038, https://doi.org/10.1029/2018MS001400, 2019.

Mitchell, B. G., Brody, E. A., Holm-Hansen, O., McClain, C., and Bishop, J.: Light limitation of phytoplankton biomass and macronutrient utilization in the Southern Ocean, Limnol. Oceanogr., 36, 1662–1677, https://doi.org/10.4319/lo.1991.36.8.1662, 1991.

Moore, C., Mills, M., Arrigo, K., Berman-Frank, I., Bopp, L., Boyd, P., Galbraith, E., Geider, R., Guieu, C., Jaccard, S., and Ulloa, O.: Processes and patterns of oceanic nutrient limitation, Nat. Geosci., 6, 701–710, https://doi.org/10.1038/ngeo1765, 2013.

Moore, J. K., Doney, S. C., Glover, D. M., and Fung, I. Y.: Iron cycling and nutrient-limitation patterns in surface waters of the World Ocean, Deep-Sea Res. Pt. II, 49, 463–507, https://doi.org/10.1016/S0967-0645(01)00109-6, 2001.

Moriarty, R. and O'Brien, T. D.: Distribution of mesozooplankton biomass in the global ocean, Earth Syst. Sci. Data, 5, 45–55, https://doi.org/10.5194/essd-5-45-2013, 2013.

Müller, W. A., Jungclaus, J. H., Mauritsen, T., Baehr, J., Bittner, M., Budich, R., Bunzel, F., Esch, M., Ghosh, R., Haak, H., and Marotzke, J.: A Higher-resolution Version of the Max Planck Institute Earth System Model (MPI-ESM1.2-HR), J. Adv. Model. Earth Sy., 10, 1383–1413, https://doi.org/10.1029/2017MS001217, 2018.

Nissen, C., Gruber, N., Münnich, M., and Vogt, M.: Southern Ocean phytoplankton community structure as a gatekeeper for global nutrient biogeochemistry, Global Biogeochem. Cy., 35, e2021GB006991, https://doi.org/10.1029/2021GB006991, 2021.

Pauly, D. and Christensen, V.: Primary production required to sustain global fisheries, Nature, 374, 255–257, https://doi.org/10.1038/374255a0, 1995.

Petrik, C., Luo, J., Heneghan, R., Everett, J., and Harrison, A.: Assessment and constraint of mesozooplankton in CMIP6 Earth system models, Global Biogeochem. Cy., 36, e2022GB007367, https://doi.org/10.1029/2022GB007367, 2022.

Petrou, K., Kranz, S. A., Trimborn, S., Hassler, C. S., Ameijeiras, S. B., Sackett, O., Ralph, P. J., and Davidson, A. T.: Southern Ocean phytoplankton physiology in a changing climate, J. Plant Physiol., 203, 135–150, https://doi.org/10.1016/j.jplph.2016.05.004, 2016.

Prowe, A. F., Visser, A. W., Andersen, K. H., Chiba, S., and Kiørboe, T.: Biogeography of zooplankton feeding strategy, Limnol. Oceanogr., 64, 661–678, https://doi.org/10.1002/lno.11067, 2019.

Prowe, A. F., Su, B., Nejstgaard, J. C., and Schartau, M.: Food web structure and intraguild predation affect ecosystem functioning in an established plankton model, Limnol. Oceanogr., 67, 843–855, https://doi.org/10.1002/lno.12039, 2022.

Ratnarajah, L., Abu-Alhaija, R., Atkinson, A., Batten, S., Bax, N. J., Bernard, K. S., Canonico, G., Cornils, A., Everett, J. D., Grigoratou, M., and Yebra, L.: Monitoring and modelling marine zooplankton in a changing climate, Nat. Commun., 14, 564, https://doi.org/10.1038/s41467-023-36241-5, 2023.

Rohr, T., Richardson, A. J., Lenton, A., Chamberlain, M. A., and Shadwick, E. H.: Zooplankton grazing is the largest source of uncertainty for marine carbon cycling in CMIP6 models, Commun. Earth Environ., 4, 212, https://doi.org/10.1038/s43247-023-00871-w, 2023.

Ryan-Keogh, T. J., Thomalla, S. J., Monteiro, P. M., and Tagliabue, A.: Multidecadal trend of increasing iron stress in Southern Ocean phytoplankton, Science, 379, 834–840, https://doi.org/10.1126/science.abl5237, 2023.

Sarmiento, J. L., Gruber, N., Brzezinski, M., and Dunne, J.: High-latitude controls of thermocline nutrients and low latitude biological productivity, Nature, 427, 56–60, https://doi.org/10.1038/nature02127, 2004a.

Sarmiento, J. L., Slater, R., Barber, R., Bopp, L., Doney, S., Hirst, A., Kleypas, J., Matear, R., Mikolajewicz, U., Monfray, P., and Stouffer, R.: Response of ocean ecosystems to climate warming, Global Biogeochem. Cy., 18, GB3003, https://doi.org/10.1029/2003GB002134, 2004b.

Séférian, R., Nabat, P., Michou, M., Saint-Martin, D., Voldoire, A., Colin, J., Decharme, B., Delire, C., Berthet, S., Chevallier, M., S., S., and Madec, G.: Evaluation of CNRM earth system model, CNRM-ESM2-1: Role of earth system processes in present-day and future climate, J. Adv. Model. Earth Sy., 11, 4182–4227, https://doi.org/10.1029/2019MS001791, 2019.

Séférian, R., Berthet, S., Yool, A., Palmieri, J., Bopp, L., Tagliabue, A., Kwiatkowski, L., Aumont, O., Christian, J., Dunne, J., and Yamamoto, A.: Tracking improvement in simulated marine biogeochemistry between CMIP5 and CMIP6, Current Climate Change Reports, 6, 95–119, https://doi.org/10.1007/s40641-020-00160-0, 2020.

Sellar, A. A., Jones, C. G., Mulcahy, J. P., Tang, Y., Yool, A., Wiltshire, A., O'connor, F. M., Stringer, M., Hill, R., Palmieri, J., and Zerroukat, M.: UKESM1: Description and evaluation of the UK Earth System Model, J. Adv. Model. Earth Sy., 11, 4513–4558, https://doi.org/10.1029/2019MS001739, 2019.

Shurin, J. B., Clasen, J. L., Greig, H. S., Kratina, P., and Thompson, P. L.: Warming shifts top-down and bottom-up control of pond food web structure and function, Philos. T. Roy. Soc. B, 367, 3008–3017, https://doi.org/10.1098/rstb.2012.0243, 2012.

Song, H., Long, M. C., Gaube, P., Frenger, I., Marshall, J., and McGillicuddy Jr, D. J.: Seasonal variation in the correlation between anomalies of sea level and chlorophyll in the Antarctic Circumpolar Current, Geophys. Res. Lett., 45, 5011–5019, https://doi.org/10.1029/2017GL076246, 2018.

Steinacher, M., Joos, F., Frölicher, T. L., Bopp, L., Cadule, P., Cocco, V., Doney, S. C., Gehlen, M., Lindsay, K., Moore, J. K.,

Schneider, B., and Segschneider, J.: Projected 21st century decrease in marine productivity: a multi-model analysis, Biogeosciences, 7, 979–1005, https://doi.org/10.5194/bg-7-979-2010, 2010.

Stock, C. A., Dunne, J. P., and John, J. G.: Drivers of trophic amplification of ocean productivity trends in a changing climate, Biogeosciences, 11, 7125–7135, https://doi.org/10.5194/bg-11-7125-2014, 2014a.

Stock, C., Dunne, J. P., and John, J. G.: Global-scale carbon and energy flows through the marine planktonic food web: An analysis with a coupled physical–biological model, Prog. Oceanogr., 120, 1–28, https://doi.org/10.1016/j.pocean.2013.07.001, 2014b.

Swart, N. C., Cole, J. N. S., Kharin, V. V., Lazare, M., Scinocca, J. F., Gillett, N. P., Anstey, J., Arora, V., Christian, J. R., Hanna, S., Jiao, Y., Lee, W. G., Majaess, F., Saenko, O. A., Seiler, C., Seinen, C., Shao, A., Sigmond, M., Solheim, L., von Salzen, K., Yang, D., and Winter, B.: The Canadian Earth System Model version 5 (CanESM5.0.3), Geosci. Model Dev., 12, 4823–4873, https://doi.org/10.5194/gmd-12-4823-2019, 2019.

Tagliabue, A., Aumont, O., DeAth, R., Dunne, J. P., Dutkiewicz, S., Galbraith, E., Misumi, K., Moore, J. K., Ridgwell, A., Sherman, E., and Yool, A.: How well do global ocean biogeochemistry models simulate dissolved iron distributions?, Global Biogeochem. Cy., 30, 149–174, https://doi.org/10.1002/2015GB005289, 2016.

Tagliabue, A., Bowie, A. R., Boyd, P. W., Buck, K. N., Johnson, K. S., and Saito, M. A.: The integral role of iron in ocean biogeochemistry, Nature, 543, 51–59, https://doi.org/10.1038/nature21058, 2017.

Tagliabue, A., Kwiatkowski, L., Bopp, L., Butenschön, M., Cheung, W., Lengaigne, M., and Vialard, J.: Persistent uncertainties in ocean net primary production climate change projections at regional scales raise challenges for assessing impacts on ecosystem services, Frontiers in Climate, p. 149, https://doi.org/10.3389/fclim.2021.738224, 2021.

Terhaar, J., Kwiatkowski, L., and Bopp, L.: Emergent constraint on Arctic Ocean acidification in the twenty-first century, Nature, 582, 379–383, https://doi.org/10.1038/s41586-020-2360-3, 2020.

Terhaar, J., Frölicher, T. L., and Joos, F.: Southern Ocean anthropogenic carbon sink constrained by sea surface salinity, Sci. Adv., 7, eabd5964, https://doi.org/10.1126/sciadv.abd5964, 2021a.

Terhaar, J., Torres, O., Bourgeois, T., and Kwiatkowski, L.: Arctic Ocean acidification over the 21st century co-driven by anthropogenic carbon increases and freshening in the CMIP6 model ensemble, Biogeosciences, 18, 2221–2240, https://doi.org/10.5194/bg-18-2221-2021, 2021b.

Terhaar, J., Frölicher, T. L., and Joos, F.: Observation-constrained estimates of the global ocean carbon sink from Earth system models, Biogeosciences, 19, 4431–4457, https://doi.org/10.5194/bg-19-4431-2022, 2022.

Tjiputra, J. F., Schwinger, J., Bentsen, M., Morée, A. L., Gao, S., Bethke, I., Heinze, C., Goris, N., Gupta, A., He, Y.-C., Olivié, D., Seland, Ø., and Schulz, M.: Ocean biogeochemistry in the Norwegian Earth System Model version 2 (NorESM2), Geosci. Model Dev., 13, 2393–2431, https://doi.org/10.5194/gmd-13-2393-2020, 2020.

Tsujino, H., Nakano, H., Sakamoto, K., Urakawa, S., Hirabara, M., Ishizaki, H., and Yamanaka, G.: Reference manual for the Meteorological Research Institute Community Ocean Model version 4 (MRI. COMv4), Technical Reports of the Meteorological Research Institute, 80, 306, 2017.

Uchida, T., Balwada, D., Abernathey, R., Prend, C. J., Boss, E., and Gille, S. T.: Southern Ocean phytoplankton blooms observed by biogeochemical floats, J. Geophys. Res.-Oceans, 124, 7328–7343, https://doi.org/10.1029/2019JC015355, 2019.

Westberry, T., Behrenfeld, M., Siegel, D., and Boss, E.: Carbon-based primary productivity modeling with vertically resolved photoacclimation, Global Biogeochem. Cy., 22, GB2024, https://doi.org/10.1029/2007GB003078, 2008.

Williamson, M. S., Thackeray, C. W., Cox, P. M., Hall, A., Huntingford, C., and Nijsse, F. J.: Emergent constraints on climate sensitivities, Rev. Mod. Phys., 93, 025004, https://doi.org/10.1103/RevModPhys.93.025004, 2021.

Woodward, S., Roberts, D., and Betts, R.: A simulation of the effect of climate change–induced desertification on mineral dust aerosol, Geophys. Res. Lett., 32, L18810, https://doi.org/10.1029/2005GL023482, 2005.

Xue, T., Frenger, I., Oschlies, A., Stock, C. A., Koeve, W., John, J. G., and Prowe, A. E.: Mixed layer depth promotes trophic amplification on a seasonal scale, Geophys. Res. Lett., 49, e2022GL098720, https://doi.org/10.1029/2022GL098720, 2022a.

Xue, T., Frenger, I., Prowe, A. E. F., José, Y. S., and Oschlies, A.: Mixed layer depth dominates over upwelling in regulating the seasonality of ecosystem functioning in the Peruvian upwelling system, Biogeosciences, 19, 455–475, https://doi.org/10.5194/bg-19-455-2022, 2022b.

Ziehn, T., Chamberlain, M. A., Law, R. M., Lenton, A., Bodman, R. W., Dix, M., Stevens, L., Wang, Y.-P., and Srbinovsky, J.: The Australian earth system model: ACCESS-ESM1.5, Journal of Southern Hemisphere Earth Systems Science, 70, 193–214, https://doi.org/10.1071/ES19035, 2020.